A New GPS Data Processing Algorithm for the Positioning of Oceanographic Experiments

KEVIN W. KEY AND GEORGE H. BORN

Colorado Center for Astrodynamics Research, University of Colorado, Boulder, Colorado

KEVIN D. LEAMAN AND PETER VERTES

Rosenstiel School of Marine and Atmospheric Science, University of Miami, Miami, Florida

(Manuscript received 31 March 1998, in final form 14 October 1998)

ABSTRACT

In this paper, the authors present a Global Positioning System (GPS) algorithm for medium accuracy (1-m rms) positioning of ocean buoys. The application addressed in this paper is that of the Fast Pegasus experiments that require the positioning of surface buoys used in collecting subsurface acoustic data for ocean current profiling. The current GPS system designed for the Fast Pegasus experiments requires a land-based single-frequency GPS receiver for differential GPS positioning. In contrast, the technique presented here is designed for the point positioning of a stand-alone single-frequency GPS receiver (which is in motion) and does not require the use of a land-based reference receiver.

The precise point positioning algorithm developed here uses postprocessed GPS satellite ephemerides and clock corrections to compute the position of a single GPS receiver. A square root information filter/smoother uses the GPS pseudorange and carrier phase measurements to estimate the position and clock offset of the receiver, 15 ionospheric coefficients from a polynomial ionospheric model, and the carrier phase ambiguities. The two major goals of this algorithm are 1) to provide 1-m (rms) absolute positions and 2) to provide 1-cm s^{-1} (rms) absolute velocities.

In three tests conducted during 1–3 August 1996, the precise point positioning algorithm computes absolute positions with an average bias of 0.396, 0.362, and −0.386 m, in the east, north and vertical directions with average standard deviations of 0.149, 0.216, and 0.484 m, respectively, when compared with carrier phase differential positions. Additionally, the precise point positioning algorithm provides velocity information that has a mean error of 0.01 cm s^{-1} in all directions with standard deviations of 0.15, 0.19, 0.37 cm s^{-1}, in the east, north and vertical directions. Based on the data collected here, the precise point positioning algorithm meets the Fast Pegasus GPS data processing requirements and should be adopted as the standard algorithm for postprocessing the Fast Pegasus GPS data. Furthermore, this algorithm eliminates the need to set up a land-based reference receiver, thereby increasing the range of Fast Pegasus experiments while at the same time decreasing the cost.

1. Introduction

The Fast Pegasus experiments are a joint project between the Rosenstiel School of Marine and Atmospheric Science (RSMAS) at the University of Miami and the Colorado Center for Astrodynamics Research (CCAR) at the University of Colorado. The purpose of the Fast Pegasus experiments is to provide velocity profiles with depth of ocean currents. The experiment consists of acoustically tracking a velocity profiler (the Fast Pegasus) from a ship and buoy (Leaman 1991; Leaman and Rocken 1994; Leaman et al. 1995). See Fig. 1 for a schematic of the current system design. Simultaneous sonar measurements at a ship and buoy provide relative positional information of a probe as it descends/ascends through the ocean. During each descent/ascent of the probe, the ship and buoy positions are determined by onboard Global Positioning System (GPS) equipment. Because the ship and buoy positions are known relative to a fixed reference frame, the velocity profile of the underlying ocean currents can be measured. RSMAS is responsible for the buoy and acoustic equipment design and CCAR is responsible for providing information on the GPS equipment and associated data reduction techniques.

There are three requirements on the GPS equipment and data processing algorithms (Key et al. 1996).

1) *100-m absolute position knowledge of the ship and buoy:* This requirement enables the buoy to be re-

Corresponding author address: Kevin W. Key, Center for Space Research, University of Texas at Austin, 3925 West Braker, Suite 200, Austin, TX 78759-5321.
E-mail: key@csr.utexas.edu

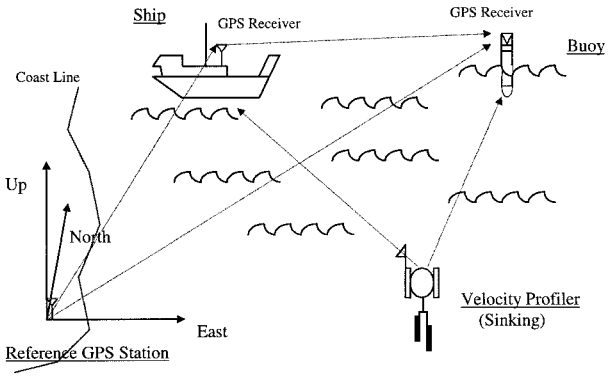

FIG. 1. A schematic of the current Fast Pegasus system design.

covered after deployment. A stand-alone, single-frequency GPS receiver has the capability of meeting this requirement. Indeed, during Fast Pegasus drops, the buoy transmits its position to the ship where it is displayed on a PC.

2) *1-m (rms) relative position knowledge between the ship and buoy:* The absolute positions of the ship and buoy are not critical. However, the distance between the two acoustic transducers must be measured accurately in order to obtain accurate subsurface velocity measurements. This requirement can be met by computing the relative position between the ship and buoy and requires that only a single-frequency GPS receiver be operated on each platform during tests (Key et al. 1996). Note that if a processing algorithm can provide 1-m (rms) absolution positions, then both requirements 1 and 2 can be met simultaneously.
3) *1-cm s^{-1} absolute velocity knowledge of the ship and buoy:* Any velocity errors introduced by the GPS solutions will be mapped directly into the subsurface current velocities. Because the noise of the acoustic equipment is about 1 cm s^{-1} (rms), the GPS equipment is required to provide the same level of precision. Key et al. (1996) demonstrated that selective availability (SA) was the driving force behind the GPS equipment selection and data processing algorithm. [SA is the intentional degradation of the GPS signals by the Department of Defense. See Leicke (1995) for a discussion of SA.] In Key et al. (1996), three single-frequency GPS receivers were required to remove the velocity influences of SA: one land-based fiducial site, one on board the ship, and one on board the buoy. The GPS data could then be processed in a differential manner to remove the unwanted effects of SA.

The requirement of a land-based fiducial site has two deleterious consequences for the Fast Pegasus experiments. First, a land-based fiducial site must be set up and accurately surveyed during Fast Pegasus experiments. It will be demonstrated later in this paper that independent fiducial sites, which collect GPS data at a slower rate than the 2-s rate of the Fast Pegasus GPS receivers, come close but do not quite meet the 1 cm s^{-1} velocity requirement. This eliminates the use of the International GPS Service for Geodynamics (IGS) network, which collects data at 30-s intervals (Beutler et al. 1995). Indeed, it may not even be possible to locate a land-based fiducial site near to probe deployments. Second, the fiducial site must record data throughout the entire time the ship is at sea because, currently, there is no cost-efficient method for turning the fiducial site on and off when acoustic data are collected. Data are collected at a 2-s interval, and experience has shown that disk space fills up quickly and that the large data files are difficult to manipulate. These practical limitations are severe enough that another method, which does not use relative positioning (but that does provide sufficient accuracy), is worth exploring.

In this paper, we will present an alternate algorithm for the location of the ship and buoy that does not require a land-based fiducial site. The method, which will be referred to as precise point positioning, uses post-processed GPS ephemerides and high-rate clock corrections to reduce the effects of SA. The algorithm is specifically designed for the single-frequency GPS receivers already in use by the Fast Pegasus experiments and is different from other precise point positioning algorithms because it uses both the carrier phase and pseudorange measurements to estimate the ionosphere as part of the navigation process. In section 2, the latest Fast Pegasus experiment, which was specifically designed to evaluate the new precise point positioning algorithm, will be detailed. This will include a discussion of the equipment used and the tests performed during the experiment. The algorithm will be presented in section 3 and results of applying the algorithm to the Fast Pegasus experiment will be presented in section 4. Finally, a discussion of the results will be given in section 5, followed by conclusions in section 6.

2. Experimental description

During 1–3 August 1996, three Fast Pegasus tests were performed at the University of Miami, which were designed to explore the accuracy of the acoustic equipment and the GPS positioning algorithm. The three tests, in chronological order, were the following.

1) On 1 August 1996, the Fast Pegasus velocity profiler was sunk and held fast at the bottom of the Atlantic Ocean (approximately 150-m depth). The probe was not released until the tests for the day were complete. Because the probe was motionless relative to the ocean, the ocean velocity profile that is recorded should show a zero velocity for the velocity profiler. Any difference from a zero velocity profile will be due to acoustic errors, GPS errors, and noise. Therefore, this test should provide information on the accuracy of the Fast Pegasus system as a whole.

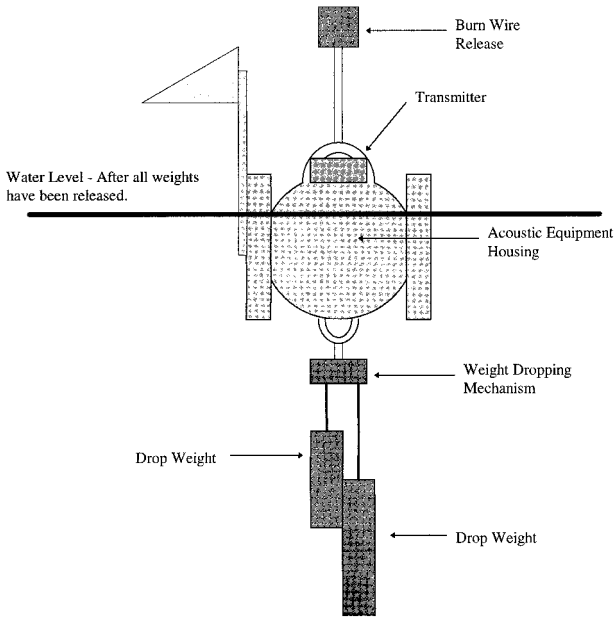

FIG. 2. The velocity profiler (Fast Pegasus).

2) On 2 August 1996, the Fast Pegasus velocity profiler was deployed three times in the Atlantic Ocean while simultaneously being tracked by a ship and buoy. The deployment was meant to demonstrate the overall ability of the Fast Pegasus system to determine the ocean velocity profile.
3) On 3 August 1996, the velocity profiler was sunk to the bottom of Biscayne Bay (approximately 10-m depth) and acoustic data were collected for a zero velocity profile (similar to the first test). This test is the same as the first test except that the shallow depth will demonstrate the effects of waves and temperature gradients at the ocean–atmosphere boundary layer. Any surface effects should be present in the signals of the acoustic equipment.

Throughout each of these tests, high rate GPS data (2-s interval) were collected from five separate GPS receivers. The receivers were arranged in such a manner that a precise point positioning algorithm could be directly compared to the currently used relative positioning algorithm. Two dual-frequency receivers were set up on board a ship and at a reference site while three single-frequency receivers (the current GPS system design) were setup on board a ship, on board a buoy, and at a reference site. The reason for setting up the extra dual-frequency receivers was so that an independent, differential, ionospheric-free, carrier phase solution could be generated as truth data for the experiment. A solution generated using the differential, ionospheric-free, carrier phase measurements requires ambiguity resolution on-the-fly and is accurate to within a few centimeters (Mader 1995).

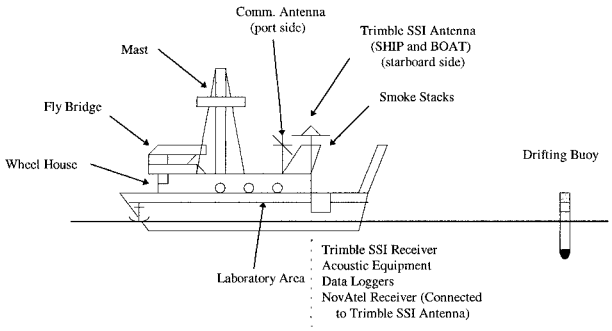

FIG. 3. The R/V *Calanus* and buoy. (See Fig. 4 for more information on the buoy design.)

a. The velocity profiler (Fast Pegasus)

The velocity profiler used in this series of Fast Pegasus tests is shown schematically in Fig. 2. The velocity profiler is a modified version of the probe presented in Leaman et al. (1995). A simple beacon-type acoustic transmitter is housed inside the velocity profiler casing. The beacon is designed to cycle through four transmit frequencies every 4 s. The transmit frequencies are 13.0, 12.5, 12.0, and 11.5 kHz with the pattern being repeated every 16 s. The transmitter clock is set to GPS time using the NovAtel receiver one pulse per second output and is not expected to drift significantly over the 1–2-h deployment time. If any drift does occur, it can be corrected upon recovery of the probe.

The velocity profiler is deployed at a particular location by the research vessel. The velocity profiler starts its descent of one to two meters per second (predefined before the test depending on the depth of the ocean) when the burn-wire release mechanism is triggered. A pressure gauge on the velocity profiler provides depth information as a function of time, which is used later in processing the acoustic data. The weights carried at the bottom of the velocity profiler provide the negative buoyancy and are released when the velocity profiler comes into contact with the ocean floor. While the velocity profiler is descending/ascending through the ocean the pings produced by the transmitter are registered and recorded by receivers at the ship and buoy (Leaman et al. 1995).

b. The ship

The Research Vessel *Calanus* (owned and operated by the University of Miami) was used to deploy the velocity profiler and the acoustic buoy, while simultaneously providing a laboratory for equipment evaluation and data collection. In these tests, the ship was taken out to sea every morning and returned before sunset. However, in operational use, the Fast Pegasus ships would remain at sea for one to two weeks.

A single Trimble Geodetic L_1/L_2 series (with a ground plane) GPS antenna was located on the starboard side of the ship (Fig. 3). A 12-channel, single-frequency

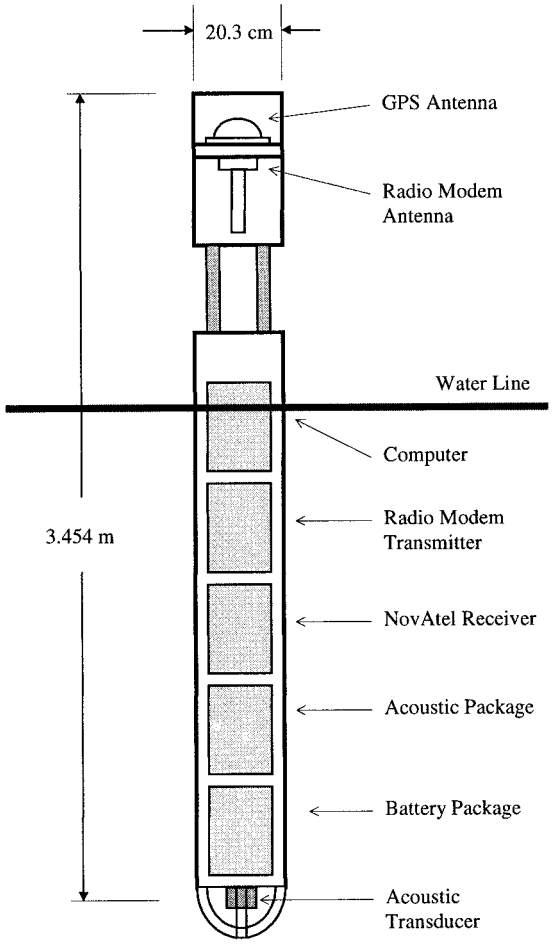

FIG. 4. The GPS/acoustic remote buoy.

NovAtel receiver and a 10-channel, dual-frequency Trimble SSI receiver were connected to the antenna via a signal splitter. (No significant loss of signal was observed with this setup.) Because of the mast and other ship structures near the antenna, the noise level of the GPS data collected during these experiments is expected to be higher than carefully chosen land-based sites due to antenna phase center scattering (Zhang and Schwarz 1996).

c. The buoy

The buoy design is a simple spar buoy with an overall length of 3.45 m. The buoy is split into two compartments (Fig. 4). The top compartment houses two antennas; a GPS NovAtel 501 antenna and a whip antenna for serial communications with the ship. The bottom compartment houses the transponder equipment, the NovAtel receiver, and batteries. The buoy is ballasted so that the antenna compartment is roughly 1.5 m out of the water at all times. The GPS receiver on board the buoy is programmed to collect data at a 2-s rate. Additionally, the receiver is programmed to send its location to an auxiliary radio modem, which then transmits the position of the buoy to the ship via the serial communications antenna (Fig. 3). A computer on board the ship keeps track of the buoy location in real time.

d. The fiducial sites

Two independent fiducial sites were surveyed at the Rosenstiel School of Marine and Atmospheric Sciences. One site was occupied by a Trimble Geodetic L_1/L_2 antenna with ground plane and the second site was occupied by a NovAtel 501 antenna. The receivers for each antenna (located on the third floor of the Marine Science Center Building) were connected to the antennas with 30 m of coaxial cable. The distance between the two antennas was approximately 10 m. Postexperiment analysis of the GPS data showed that multipath was high at the top of the building and was most likely due to a large metallic chimney on the top of the building.

The coordinates of each antenna phase center were determined using the Jet Propulsion Laboratory's (JPL) GPS Inferred Positioning System (GIPSY) software (Lichten 1990). Two fiducial sites, located at Richmond, Florida, and Miami, Florida, were used as references for the calculations. These two sites are operated by the IGS and their positions are known accurately (Beutler et al. 1995). Postprocessed precise orbits by JPL were used for the GPS ephemerides (Lichten and Border 1987). Both pseudoranges and carrier phase data were used in the computations and the calculated positions have an estimated uncertainty of a few centimeters.

e. The Fast Pegasus procedure

The general Fast Pegasus experimental procedure is as follows. 1) The buoy is deployed prior to launching the velocity profiler. 2) The velocity profiler is deployed. 3) The ship is positioned and stopped. 4) The profiler is released from the ocean's surface using a burn wire release. 5) Both the ship and buoy record the time of arrival of the pings produced by the velocity profiler. Simultaneously, GPS data are collected. 6) When the velocity profiler reaches the bottom, weights are dropped and the profiler ascends through the ocean. 7) The velocity profiler is recovered by the ship and reset for another drop. 8) When the day's tests are complete the buoy is recovered by the ship.

The accumulated data consist of positions for the two surface locations (ship and buoy) as determined by GPS every 2 s and apparent one-way travel times for the acoustic pings from the profiler to each of the two surface locations every 4 s. GPS positions are smoothed and subsampled at the 4-s rate, taking into account the correction required for the difference in time between when an acoustic pulse was transmitted and when it was received by the ship or the buoy. Any required clock corrections to the buoy, ship, and profiler are applied.

Bad acoustic travel times are identified and edited from the data stream. Profiler depth is determined using time from surface release or bottom turnaround, the known fall (or ascent) rate of the profiler, and the water depth. Acoustic travel times are converted to slant ranges between the profiler and the buoy or the ship using the vertical sound speed profile appropriate to the area. The time history of horizontal (east–north) profiler displacements for a given drop can then be determined trigonometrically by removing the probe depth and adding the probe locations relative to the ship–buoy coordinates to the positions of the ship–buoy coordinate system as determined by GPS. A least squares linear running fit to the east and north displacements over a limited number of points (usually 10–15) is then made to the east and north displacements and the slope of that fit is taken as the estimated absolute velocity.

3. The precise point positioning algorithm

Precise point positioning is defined as the computation of the position of a single stand-alone GPS receiver using postexperiment precise orbits and clock corrections. The major error sources of point positioning in real time (no precise point positioning) are GPS clock and orbital errors (the major contribution being SA), atmospheric attenuation errors (both the ionosphere and the troposphere), and receiver errors (multipath and measurement noise). When SA is off, the position of the receiver can be computed with an error of 30 m (approximate 3D error, 95% of the time). When SA is on, the position of a receiver can be computed with an error of 156 m (approximate 3D error, 95% of the time). When precise orbit and clock corrections are used, the greatest error sources in precise point positioning become the atmospheric errors because orbital errors and SA are virtually eliminated. Thus, given that the atmospheric error sources can be modeled accurately, postexperiment, submeter accurate positioning with precise orbits and clock corrections is a real possibility.

a. Precise point positioning

The most widely used method for the reduction of SA (and other GPS error sources) is differential GPS. However, in recent years, highly accurate GPS satellite ephemerides and clock corrections have been generated by various agencies using a permanent GPS tracking network. Currently, the ephemerides can be estimated to an uncertainty of 15 cm and the clock corrections can be estimated to an uncertainty of 1 ns (Mireault et al. 1995). Therefore, an alternate method for the reduction of SA errors is precise point positioning, which uses the post processed GPS orbits and clock corrections, instead of the broadcast orbits and clock parameters transmitted by the GPS satellites. Precise point positioning with pseudorange data from a single-frequency GPS receiver can provide 1-m (rms) horizontal accuracy and 2-m (rms) vertical accuracy (Lachapelle et al. 1996).[1] In Lachapelle et al. (1996) the ionosphere was accounted for by using dual-frequency GPS data from a fiducial network to correct the single-frequency GPS data. In the algorithm presented here, the carrier phase data, in combination with the pseudorange data, are used to estimate the ionosphere and thereby increase the absolute accuracy of positions to 1-m (rms) in the horizontal and vertical directions.

Typically, the GPS precise ephemerides are published in tabular format at a 15-min interval. An 11th order polynomial can be used to interpolate the Cartesian coordinates of each GPS satellite to an absolute accuracy $<$10 cm. The reference frame in which the GPS orbits are reported is the International Terrestrial Reference Frame, which is referred to a specific epoch and is realized by the position and velocity of a permanent network of global stations (IERS Conventions 1996).[2] Similarly, the satellite clock offsets are tabularized at a 30-s interval and can be interpolated to the nanosecond level using a fifth-order polynomial (Lachapelle et al. 1994). When using both precise GPS ephemerides and precise GPS clock corrections, errors associated with SA are significantly reduced (i.e., $<$30 cm).

Corrections ($\sim$2 m) must be applied to the pseudorange and carrier phase data when performing precise point positioning. First, a correction has to be applied to the GPS satellite clock corrections because a relativistic effect caused by the ellipticity of the GPS orbits is not accounted for in the postprocessed GPS clock corrections. Second, a correction has to be applied for the displacement of the antenna phase center of the GPS satellites relative to the GPS satellite center of mass.

b. The precise point positioning procedure

The procedure for analysis of the Fast Pegasus GPS data has three steps.

1) *Inspect the GPS data for cycle slips and outliers:* Because the precise point positioning method uses the L_1 carrier phase data, cycle slip detection is very important. Code has been developed that examines a linear combination of the C/A pseudorange and the L_1 carrier phase data for cycle slips. The combination has the important property that only the effects of the ionosphere and the carrier phase ambiguities remain. Because the ionosphere affects the GPS signals at low frequencies, a subtractive filter (which acts like a high-pass filter) will detect any sudden jumps in the carrier phase data due to cycle slips (Hofmann-

[1] In general, the vertical estimates will be less accurate because of the shape of the standard error ellipse and because the errors in the ionospheric and tropospheric delays map directly into the vertical component.

[2] WGS84, which is the coordinate system of the broadcast orbits, is consistent with ITRF to 0.01 ppm (Malys and Slater 1994).

Wellenhof et al. 1992). One important limitation of this linear combination is that the noise in the C/A measurement can be greater than an equivalent cycle slip of one or two cycles. Thus, small cycle slips will be undetected with this method (but will not prevent the precise point positioning algorithm from meeting the accuracy requirements of this application).

2) *Generate an a priori solution for the ship and buoy:* Because the ship and buoy can drift up to several kilometers during a typical Fast Pegasus test, an a priori solution is used to initialize the filter/smoother estimates.[3] The a priori solution need not be highly accurate (5–10 m) and a precise point position solution using only the C/A pseudorange measurements without an ionospheric model is sufficient as a starting point for the filter/smoother. This step does not contain any estimation of nuance parameters and is essentially reconstructing the positions that were generated by the receiver when it was in the field.
3) *Run the filter/smoother on the data:* A computer program named Kinematic Single Frequency (KSF) has been developed based on the square root information filter/smoother of Bierman (1977). The filter uses the GPS pseudorange and carrier phase measurements to estimate the various parameters associated with each measurement type. See the appendix for a description of how the measurements are modeled. The position of the receiver is modeled as a random walk stochastic process and the clock offset of the receiver is modeled as a white noise stochastic process (Bierman 1977). The positions of the GPS satellites are not estimated and are taken from the precise ephemeris. Similarly, the GPS clock offsets are not estimated and are taken from the precise clock corrections. In addition to the position and clock offset of the receiver, the filter estimates the 15 coefficients of a polynomial ionospheric model (see the appendix) and the carrier phase ambiguities as bias parameters. Suggested a priori estimates and uncertainties are given in Table 1. The estimates and uncertainties are based on the fact that the data have been adjusted by an approximate carrier phase ambiguity in step 1 and that initial positions and clock corrections have been generated in step 2.

These three steps are general enough that they can be used for any moving, oceanographic platform located at any place on the earth. There have been no assumptions about the rate at which data are collected except that the algorithms have been optimized for high rate data, that is, 0.5-s intervals to 10-s intervals, and the output from this algorithm is an optimal estimate of the position at each epoch of data.

TABLE 1. Suggested a priori estimates and uncertainties for the precise point positioning algorithm.

Parameter	A priori estimate	A priori uncertainty
X, Y, Z, dT_i	Single frequency point position	5.0 m
A_1	3.0 m	2.0 m
A_2–A_3	0.0 m deg^{-1}	0.1 m deg^{-1}
A_4–A_6	0.0 m deg^{-2}	0.05 m deg^{-2}
A_7–A_{10}	0.0 m deg^{-3}	0.01 m deg^{-3}
A_{11}–A_{15}	0.0 m deg^{-4}	0.001 m deg^{-4}
N_i^j	0 cycles	10 cycles

4. Results

All GPS positions (both precise point positions and precise relative positions) have been computed using the software KSF. KSF has been in development at the Colorado Center for Astrodynamics Research for four years and was originally intended to be used for single-frequency data collected in a differential manner. In the differential mode, either L_1 pseudorange or L_1 carrier phase data (L_2 data, if available, can be used to compute an ionospheric correction and/or help in the resolution of ambiguities) can be used to compute an epoch-by-epoch position. The carrier phase ambiguities are resolved on the fly by means of a positional search algorithm (Remondi 1991). The GPS orbits and clock corrections are not estimated and are taken either from the broadcast navigation message or from postprocessed precise data. The software has shown to give similar results to other postprocessing geodetic–kinematic software [e.g., JPL's GIPSY software and the National Oceanic and Atmospheric Administration's Kinematic and Rapid Static software (Mader 1995)].

a. Performance of the precise point positioning algorithm

The precise point positioning algorithm described above (and detailed in the appendix) was used to compute the position of the ship and buoy during the tests of 1–3 August 1996 off the coast of Miami. Specifically, the times of the tests were as follows: (test 1) 1545–1700 UTC, 1 August 1996; (test 2) 1720–1900 UTC, 2 August 1996; and (test 3) 1500–1700 UTC, 3 August 1996. JPL precise orbits and clock corrections were used while computing the precise point positions. The a priori estimates and uncertainties of the various parameters are given in Table 1.

In addition to the precise point position solutions, differential carrier phase solutions were generated for each of the tests, except for the buoy during test 2 because of a failure to resolve ambiguities correctly. The carrier phase solutions should be accurate to a few cen-

[3] This step is based on the generality that, when using a filter to estimate parameters, a relatively good starting point produces a more accurate estimate than a relatively poor starting point. For example, using an a priori position with a 1-km error produces a less accurate estimate when compared to the position estimate based on an a priori position with a 1-m error.

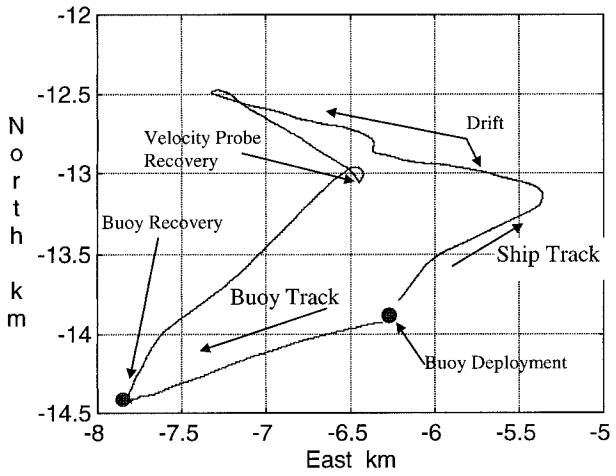

FIG. 5. The paths of the ship and buoy during test 3 on 3 Aug 1996 from 1500 to 1700 UTC. The origin of the plot is the Marine Science Center at the University of Miami.

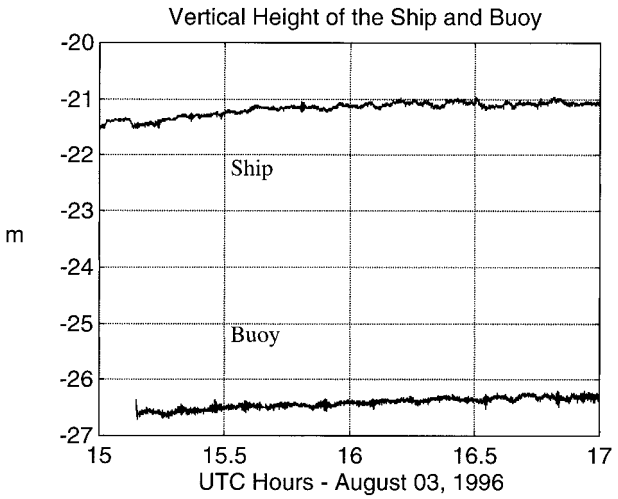

FIG. 6. The vertical height (WGS 84 Ellipsoid) of the ship and buoy during test 3 on 3 Aug 1996.

timeters; therefore, these solutions will be considered as the ''truth'' and will be used to assess the accuracy of the precise point positioning algorithm. As an example of the carrier phase solutions, Figs. 5 and 6 show the location of the buoy and ship during test 3. The bias between the two vertical measurements in Fig. 6 is due to the different antenna heights above the ocean's surface (see Fig. 3).

The polynomial ionospheric model (appendix) was tested with static data collected by the NovAtel receiver located at the fiducial site. Because dual-frequency data were also collected at the fiducial site, a direct measure of the line-of-sight ionospheric error was recorded by the dual-frequency carrier phase measurements. The NovAtel pseudorange and carrier phase data collected from test 3 (3 August 1996) were used to compute the coefficients of the ionospheric polynomial (i.e., A_1–A_{15}). When the polynomial model was compared to the carrier phase dual-frequency measurements of the ionosphere, a $\pm$15-cm difference over two hours was observed after all biases were removed. The carrier phase ambiguities are highly correlated with the A_1 term (constant bias term of the polynomial; see the appendix) in the polynomial, which means that the filter is incapable of separating estimates of the carrier phase ambiguities and the A_1 term. The conclusion of this test is that the model does recover the gradient of the ionosphere and, therefore, should introduce only minimal velocity errors into the Fast Pegasus experiments.

Before the velocity was computed, a digital low-pass filter was applied to the latitude, longitude, and height of the ship and the buoy. The filter employed was a Savitzky–Golay digital smoothing polynomial type filter. The filter uses 30 data points (which represent a smoothing window of 60 s) and a first-degree polynomial to generate a response function. The response function can be convolved with the latitude, longitude, and height components with the result of smoothing the overall position but retaining the 2-s spacing. The smoothing is comparable to the actual Fast Pegasus velocity determination algorithm, in which roughly 60 s of data are used to estimate a velocity. After the low-pass filter is run on the positional data, the velocity can be computed using a forward finite-difference approximation from the position data.

The position and velocity error for the ship on 3 August 1996 (test 3) are shown in Figs. 7 and 8. These graphs are typical of the errors in the precise point position algorithm during these sets of tests.[4] For this ex-

[4] Note that these plots reflect the overall quality of the algorithm because any errors introduced by the ''truth'' solution are very small in comparison to the errors of this algorithm.

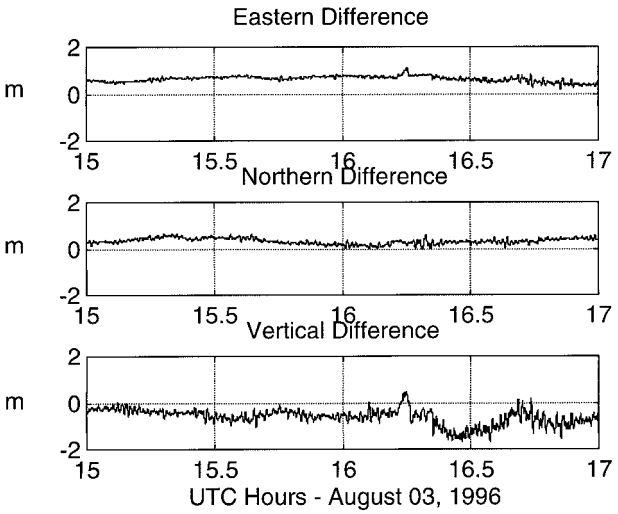

FIG. 7. The position error of the precise point positioning algorithm for test 3 on 3 Aug 1996 (ship).

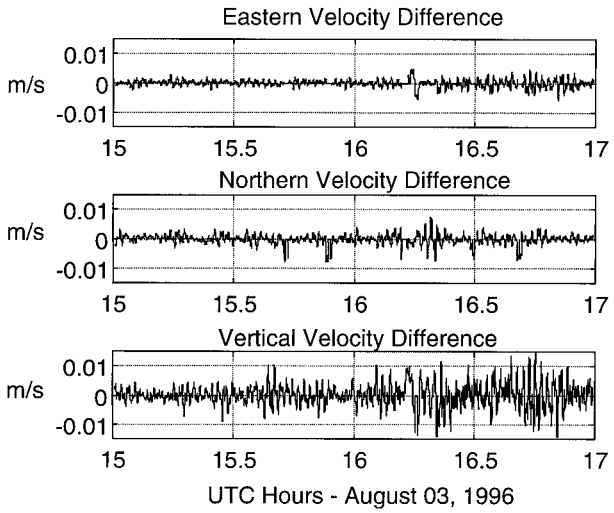

FIG. 8. The vertical velocity error of the precise point positioning algorithm for test 3 on 3 Aug 1996 (ship). The standard deviation of each plot is shown in Table 2.

ample, the rms of the postfit residuals was 0.678, 0.073, and 0.482 m for the pseudorange measurements, for the carrier phase measurements, and for all the measurements, respectively. Additionally, the approximate chi-square value (defined as the sum of square of the postfit residuals divided by the total degrees of freedom) was 0.322. This indicates that there were enough data to estimate all the parameters in the precise point positioning algorithm (because the value is less than 1.0).

The mean position errors and the standard deviation of the velocity errors are shown in Table 2 for tests 1–3. Figures 7 and 8 are typical examples of the solution errors found in Table 2. The average bias of the positional errors is 0.396, 0.362, and −0.386 m in the east, north, and vertical directions, respectively. The average standard deviations of the velocity errors are 0.15, 0.19, and 0.37 cm s^{-1} in the east, north, and vertical directions, respectively. In all cases the mean velocity error was approximately 0.01 cm s^{-1}. No comparison was made for the buoy during test 2 because KSF failed to resolve the differential carrier phase ambiguities (most likely due to the high multipath at the fiducial site) and therefore a ''truth'' could not be generated. The high vertical velocity errors can be attributed to errors in the ionospheric and tropospheric model, which map directly into the vertical component of the positions and therefore affect the vertical velocity.

b. Noise level of the acoustic equipment

Previous work with Pegasus probes using acoustic transponders deployed and accurately surveyed on the ocean bottom suggest that velocities can be determined to better than 1 m s^{-1} (Leaman and Vertes 1983; Leaman et al. 1987). Acoustic range resolution is about 1.5 cm at 1500 m s^{-1} sound speed and noise is primarily caused by small-scale perturbations in the sound–speed profile, such as those caused by internal waves or turbulence. In some isolated cases acoustic ranges are compromised not by random errors but rather by systematic errors in computing the sound ray paths. In particular, erroneous results can be obtained near the ocean bottom if ray paths intersect the bottom. Fortunately, such errors are easily detected and corrected.

5. Discussion

The combination of the pseudorange and carrier phase measurements in the precise point positioning algorithm necessitates a weighting scheme in the filter because there is a large measurement noise difference between the two types of measurements. Usually in state estimation algorithms, the standard deviation of the noise of each measurement is used to weight the partials and residuals in the filter. For example, the standard deviation of the pseudorange measurements is 0.3 m and the standard deviation for the carrier phase measurements is 0.002 m, the appropriate weighting ratio should be 1 to 150. (In other words, the carrier phase data have 1/150

TABLE 2. Position and velocity errors for the precise point positioning algorithm.

	Mean positional error*			Standard deviation of velocity error**		
	East (m)	North (m)	Vertical (m)	East (cm s^{-1})	North (cm s^{-1})	Vertical (cm s^{-1})
Test 1: Ship	1.154	0.585	−0.412	0.11	0.20	0.41
Test 1: Buoy	−0.564	0.543	−0.052	0.22	0.29	0.43
Test 2: Ship	−0.081	0.147	−0.550	0.10	0.11	0.25
Test 2: Buoy	—	—	—	—	—	—
Test 3: Ship	0.632	0.327	−0.607	0.20	0.20	0.37
Test 3: Buoy	0.838	0.207	−0.307	0.13	0.15	0.37
Average	0.396	0.362	−0.386	0.15	0.19	0.37

* The standard deviations of the positional errors were less than 0.43 m, except for test 2 (buoy) and test 3 (buoy), which had vertical standard deviations of 0.85 and 0.54 m, respectively.

** The mean velocity error was approximately 0.01 cm s^{-1} for all cases.

the amount of noise of the pseudorange measurements.)[5] However, in the case of this study, the weighting ratio of 1 to 150 was found to give erroneous answers when compared with the truth dataset. It was found that any ratio larger than 1 to 15 appears to de-weight the pseudorange measurements too much and the carrier phase ambiguities and the A_1 ionospheric bias term are not bounded, resulting in solutions with 10-m vertical errors. It is recommended that a ratio of 1 to 10 be used as the default weighting ratio.

The instantaneous accuracy of the precise point position algorithm was very dependent on the geometry of the GPS satellite constellation. A high geometric dilution of precision (GDOP) has the effect of increasing the noise on the precise point positions and, therefore, increasing noise on the velocities. The effect is illustrated in Table 2. During the later part of tests 1 and 3 (both test periods included data during the hours 1630–1700), the GDOP reached as high as 10. When the vertical velocity errors are compared with test 2 (taken later in the day; therefore, there was a different satellite geometry), a noticeable difference is apparent. Thus, when the GDOP values are around 2–5, the vertical velocity errors are 0.2 cm s^{-1} less than when the GDOP is greater than 8. One should note that a high GDOP implies only a noisy solution (and therefore a noisy velocity) and should not seriously affect the bias about a truth solution.

In addition to the precise point positioning algorithm, an alternate algorithm, which uses differential positioning and GPS data collected from a network of IGS stations, was investigated. The IGS stations record data at 30-s intervals that could be used to position the ship and buoy. Although the GPS positions would be at a slower rate than the desired 2-s interval, interpolation could be used to estimate the positions of the receivers at the 2-s rate. GPS data were obtained from the IGS site at Richmond, Florida (i.e., RCM5, the same site that was used to position the fiducial sites), during Fast Pegasus test 2 on 2 August 1996. The position of the ship was computed using the pseudorange data and the current Fast Pegasus GPS data processing algorithm. The resulting positions were smoothed using the digital polynomial filter described above, linearly interpolated to 2-s intervals and compared against the carrier phase solution. The standard deviation of the velocity errors was 0.954, 0.747, and 1.682 cm s^{-1} in the east, north, and vertical directions, respectively. Clearly, the 2-s linearly interpolated positions do not meet the Fast Pegasus requirements. However, they do come close to meeting the requirements and this technique should be considered as a backup algorithm to the precise point positioning algorithm if, for some reason, the precise orbit or clock information is not available.

The precise point positioning algorithm, as it is developed here, is not only applicable to the Fast Pegasus experiments but can also be applied to other oceanographic studies where equipment location is desired to 1-m rms at any high rate interval. Indeed, the technique has been broadly designed for the location of any moving platform, be it on land, air, or water.

6. Conclusions

The main objective of the Fast Pegasus experiment described here was to determine an alternative GPS positioning algorithm that would provide meter-level position accuracies with velocity accuracies better than 1 cm s^{-1} for floating platforms. The results from a 3-day experiment off the coast of Florida demonstrate that the precise point positioning algorithm does provide solutions that meet these requirements.

Most of the positional error in the precise point positions was in the longitudinal and vertical directions. The vertical error is most likely due to the inaccuracy of the ionospheric and tropospheric models. Both of these atmospheric error sources map directly into the vertical component of the GPS position. The longitudinal error, which was as high as 1.154 m during one test (test 1 for the ship on 1 August 1996), is more difficult to explain and is currently under investigation. The position derived velocity was shown to be well within the 1-cm s^{-1} requirement for the Fast Pegasus experiments.

The theoretical limit of precise point positioning is defined by the accuracy of the precise orbit and clock corrections, which are presently accurate to 15-cm rms and 1-ns (30 cm) rms, respectively. Thus, future work should include the reduction of all errors to that limit. For example, the polynomial ionospheric model presented here (see the appendix) could be modified to include the variations of the total electron content (TEC) shell height across different latitudes and longitudes. Or, the polynomial model could be substituted with one of the postprocessed ionospheric TEC models, for example, the IRI-95 or PRISM models (Daniell et al. 1993; Bilitza et al. 1993). In addition to modifying the ionospheric model, the zenith tropospheric delay could be estimated as part of the filter/smoother process, instead of being held fixed as is currently the case. It is difficult to state how much improvement any of these modifications would have without implementing them; however, with careful modeling and implementation, a 30-cm rms accuracy level (or better with increased accuracy of postprocessed GPS orbits and clock corrections) should be attainable in the near future.

Acknowledgments. The authors wish to thank the captain and mate of the *Calanus,* as well as the ocean technicians of RSMAS for their help in gathering the data

[5] See Bierman (1977, section III.5) for a discussion of weighting the least squares problem when more than two types of observations are used.

used in this paper. This work was supported by the National Science Foundation under Contracts OCE-9103905 and OCE-9403478.

APPENDIX

Data Models for the Precise Point Positioning Algorithm

This algorithm assumes that the receivers in use are capable of producing raw data that are being used to determine a real-time stand-alone navigation solution. The data collected and recorded in the field are generally in a binary or proprietary format and can be converted to a receiver independent exchange (RINEX) format (Gurtner 1995) when postprocessing of the data is desired. The RINEX format is designed to be general and contains header information on the particular type of receiver/antenna used, followed with the data recorded during deployment. The GPS RINEX data epoch consists of a time stamp followed by pseudorange and carrier phase measurements for each satellite being tracked at that time. The interval between epochs for kinematic experiments is usually high rate (1–5 s) and requires large amounts of electronic storage. Once the data are collected, they may be analyzed with different algorithms. The particular algorithm used in this study is presented below.

The GPS pseudorange and carrier phase measurements at one epoch t_i, for one satellite j, and one receiver i, can be modeled as (Leicke 1995)

$$\mathrm{PR}_i^j = \rho_i^j + (c - \dot{\rho}_i^j)dt_i - cdt^j + dI_i^j + dT_i^j \quad \text{(A1)}$$

$$\Phi_i^j = \rho_i^j + (c - \dot{\rho}_i^j)dt_i - cdt^j - dI_i^j + dT_i^j + \lambda N_i^j, \quad \text{(A2)}$$

where PR is the pseudorange measurement (m) from receiver i to satellite j, Φ is the carrier phase measurement (m) from receiver i to satellite j, ρ is the geometric distance (m) between receiver i and satellite j, c is the speed of light (m s^{-1}), $\dot{\rho}$ is the rate of change of the geometric distance (m s^{-1}) between receiver i and satellite j, dt_i is the receiver clock offset (s), dt^j is the satellite clock offset (s), dI is the ionospheric correction (m) from receiver i to satellite j, dT is the tropospheric correction (m) from receiver i to satellite j, and N is the carrier phase ambiguity (cycles) associated with receiver i and satellite j. The geometric distance is

$$\rho_i^j = |\boldsymbol{\rho}_i^j| = [(X^j - X_i)^2 + (Y^j - Y_i)^2 + (Z^j - Z_i)^2]^{1/2} \quad \text{(A3)}$$

and the rate of change of the geometric distance is given by

$$\dot{\rho}_i^j = \frac{\boldsymbol{\rho}_i^j \cdot \mathbf{v}_i^j}{\|\boldsymbol{\rho}_i^j\|} = \frac{(X^j - X_i)(V_x^j - V_{X_i}) + (Y^j - Y_i)(V_Y^j - V_{Y_i}) + (Z^j - Z_i)(V_Z^j - V_{Z_i})}{\rho_i^j}, \quad \text{(A4)}$$

where X, Y, and Z are the earth-centered, earth-fixed Cartesian coordinates of the receiver and satellite and V_x, V_y, and V_z are the respective velocities in the same coordinate system. Each of the Cartesian coordinates of the receiver is modeled as random walk stochastic parameter. A random walk stochastic parameter is a highly correlated estimate that depends heavily on the values of past and future estimates. The position of the satellites are interpolated from tabulated precise ephemeris tables. The receiver clock offset dt_i is estimated as white noise stochastic process. A white noise process parameter is an estimate that does not depend on past or future estimates. The satellite clock offset dt^j is interpolated from precise clock corrections table. The velocities of both the receiver and satellite can be estimated by differencing the positions from one epoch to the next.

The ionospheric correction dI is modeled as fourth-order polynomial based on the ionospheric intercept point of the satellite. The model is derived from Qiu et al. (1995) and is

$$dI_i^j = O_e(A_1 + A_2\phi + A_3\lambda + A_4\phi^2 + A_5\phi\lambda + A_6\lambda^2 + A_7\phi^3 + A_8\phi^2\lambda + A_9\phi\lambda^2 + A_{10}\lambda^3 + A_{11}\phi^4 + A_{12}\phi^3\lambda + A_{13}\phi^2\lambda^2 + A_{14}\phi\lambda^3 + A_{15}\lambda^4), \quad \text{(A5)}$$

where A_1–A_{15} are coefficients, O_e is the obliquity factor (i.e., converts the zenith delay to a line-of-sight delay; Klobuchar 1987), and ϕ and λ are the modified ionospheric intercept points defined by

$$\phi = \phi_I - \phi_0 \quad \text{and} \quad \lambda = \lambda_I - \lambda_0, \quad \text{(A6)}$$

where ϕ_I and λ_I are the ionospheric intercept points (Klobuchar 1987) and ϕ_0 and λ_0 are an initial latitude and longitude at the start of an experiment. The 15 constant coefficients can be estimated as bias parameters and the intercept ionospheric point is determined by the time and location of the GPS satellite relative to the receiver. The obliquity factor O_e assumes a fixed shell height, and 350 km was used in these experiments. Future work could include the modeling of the obliquity factor as a function of latitude versus shell height in order to create a more realistic ionospheric model.

The tropospheric correction dT is calculated from empirical models based on the temperature, pressure, and relative humidity at the time of the experiment. The zenith delay is calculated using a modified Saastamoinen model (Saastamoinen 1972) and the zenith delay is converted to a line-of-sight delay by the Niell mapping function (Niell 1996). Multipath is not accounted for in this model.

REFERENCES

Beutler, G., I. I. Mueller, and R. E. Neilan, 1995: The International GPS Service for geodynamics (IGS): The story. *GPS Trends in Precise Terrestrial, Airborne, and Spaceborne Applications*, IUGG/IAG, 3–13.

Bierman, G. J., 1977: *Factorization Methods for Discrete Sequential Estimation.* Academic Press, 241 pp.

Bilitza, D., K. Rawer, L. Bossy, and T. Gulyaeva, 1993: International reference ionosphere—Past, present, and future. *Adv. Space Res.*, **13,** 3–23.

Daniell, R. E., W. G. Whartenby, and L. D. Brown, 1993: Algorithm description for the parameterized real-time ionospheric specification model, Version 1.2. Computational Physics Inc.

Gutner, W., 1995: RINEX: The receiver independent exchange format, Version 2. Astronomical Institute, University of Bern, 18 pp. [Available online at http://www.unavco.ucar.edu/data/docs/rinex2.txt.]

Hofmann-Wellenhof, B., H. Lichtenegger, and J. Collins, 1992: *GPS Theory and Practice.* 2d ed. Springer-Verlag, 326 pp.

Key, K., S. Anderson, P. Axelrad, P. MacDoran, and G. Born, 1996: Analysis of Fast Pegasus GPS equipment and algorithms. Colorado Center for Astrodynamics Research, University of Colorado, CCAR Rep. 96-032, 27 pp.

Klobuchar, J. A., 1987: Ionospheric time-delay algorithm for single-frequency GPS users. *IEEE Trans. Aerosp. Electron. Syst.,* **AES-23,** 325–331.

Lachapelle, G., R. Klukas, D. Roberts, and W. Qiu, 1994: One-meter level kinematic point positioning using precise orbits and satellite clock corrections. *Proceedings of ION GPS-94,* ION, 1435–1443.

——, M. E. Cannon, W. Qiu, and C. Varner, 1996: Precise aircraft single-point positioning using GPS post-mission orbits and satellite clock corrections. *J. Geod.,* **70,** 562–571.

Leaman, K. D., 1991: The use of electronic aids to navigation (GPS) to improve absolute and relative vertical current profiler measurements from ships. *Proc. Int. Symp. on Marine Positioning,* Miami, FL, Marine Technology Society, 460–471.

——, and P. S. Vertes, 1983: The Subtropical Atlantic Climate Study (STACS) 1982: Summary of RSMAS PEGASUS observations in the Florida Straits. University of Miami RSMAS Tech. Rep. 83012, 154 pp. [Available from University of Miami, RSMAS, 4600 Rickenbacker Causeway, Miami, FL 33149-1098.]

——, and C. Rocken, 1994: Fast Pegasus: An ocean current profiler using combined GPS and acoustical navigation—Results of a feasibility study. *Eos, Trans. Amer. Geophys. Union,* **75,** 41 pp.

——, R. L. Molinari, and P. S. Vertes, 1987: Structure and variability of the Florida Current at 27°N: April 1982–July 1984. *J. Phys. Oceanogr.,* **17,** 565–583.

——, P. S. Vertes, and C. Rocken, 1995: Polaris: A GPS-navigated ocean acoustic current profiler. *J. Atmos. Oceanic Technol.,* **12,** 541–549.

Leick, A., 1995: *GPS Satellite Surveying.* John Wiley and Sons, 560 pp.

Lichten, S. M., 1990: Estimation and filtering for high-precision GPS positioning applications. *Manuscr. Geodaet.,* **15,** 159–176.

——, and J. S. Border, 1987: Strategies for high-precision global positioning system orbit determination. *J. Geophys. Res.,* **92** (B12), 12 751–12 762.

Mader, G. L., 1995: Kinematic and Rapid Static (KARS) GPS positioning: Techniques and recent experiences. *GPS Trends in Precise Terrestrial, Airborne, and Spaceborne Applications*, IAG Symposium 115, IAG, 170–174.

Malys, S., and J. Slater, 1994: Maintenance and enhancement of the World Geodetic System. *Proc. ION GPS-94,* ION, 17–24.

McCarthy, D. D., 1996: IERS Conventions 1996. IERS Tech. Note 21, U.S. Naval Observatory, 95 pp. [Available online at http://maia.nsno.navy.mil/conventions.html.]

Mireault, Y., J. Kouba, and F. Lahaye, 1995: IGS Combination of Precise GPS Satellite Ephemerides and Clocks. *GPS Trends in Precise Terrestrial, Airborne, and Spaceborne Applications,* IUGG/IAG, 14–23.

Niell, A. E., 1996: Global mapping function for the atmosphere delay at radio wavelengths. *J. Geophys. Res.,* **101** (B2), 3227–3246.

Qiu, W., G. Lachapelle, and M. E. Cannon, 1995: Ionospheric effect modeling for single frequency GPS users. *Manuscr. Geodaet.,* **20,** 96–109.

Remondi, B. W., 1991: Kinematic GPS results without static initialization. NOAA Tech. Memo. NOS (NGS-55), 25 pp.

Saastamoinen, J., 1972: Atmospheric correction for the troposphere and stratosphere in radio ranging of satellites. *The Use of Artificial Satellites for Geodesy, Geophys. Monogr.,* No. 15, Amer. Geophys. Union, 247–251.

Zhang, Q., and K. Schwarz, 1996: Estimating double difference GPS mulitpath under kinematic conditions. *Position Location and Navigation Symposium,* IEEE PLANS'96, 285–291.